J Mater Sci: Mater Electron (2023) 34:585

Structural and electrical property characterization of thermoelectric ($Ca_3Co_4O_{9\pm\delta}$) ceramic oxide fabrication by various reducing agent method

Jothi Ramalingam Rajabathar[1,*], Radhika Thankappan[2,3,*], Hamad AL-Lohedan[1], and Hassan A. Al-Sigh[1,3]

[1] Chemistry Department, College of Science, King Saud University, P.O. Box 2455, Riyadh 11451, Saudi Arabia
[2] C-MET, Center for Materials for Electronics Technology, Athani, M.G. Kavu P.O., Thrissur, Kerala 680581, India
[3] Department of VLSI Microelectronics, Institute of ECE, Saveetha School of Engineering, SIMATS, Chennai 602105, India

Received: 15 December 2022
Accepted: 25 January 2023
Published online: 21 February 2023

ABSTRACT

In the present study, calcium cobalt oxide-based ceramic oxide ($Ca_3Co_4O_{9\pm\delta}$) is synthesized by various reducing agent method by metal complex-assisted sol–gel assisted followed by combustion method using various reducing agents. The reducing agents adopted in the study are citric acid, starch polymer, and polyethylene glycol. The detailed structural and surface characterizations of as-prepared $Ca_3Co_4O_{9+\delta}$ have demonstrated by XRD, TGA, and diffuse UV–visible spectral analysis. Hydrothermal method-prepared Iron-doped $Ca_3Co_4O_{9\pm\ \delta}$ ceramic shows the Nanorods' morphology. Electrical properties such as conductivity, Hall co-efficient, and electron mobility studies have been demonstrated. The density of the prepared materials by changing the stoichiometry ranges from 2.72 g/cm^3 (relative density 55%) to 2.91 g/cm^3 (relative density 58.9%). The density is found to be improved by decreasing the amount of calcium. The higher density is obtained for $Ca_{2.90}$ $Co_{3.91}O_{9\pm\delta}$ which is 2.91 g/cm^3 (58.9% of theoretical density). The effect of foreign metal ion doping in bulk calcium carbonate has studied and compared their electronic properties. The various reducing agent method-prepared $Ca_3Co_4O_{9\pm\delta}$ shows the promising thermoelectric features. Polymer method-prepared $Ca_3Co_4O_{9\pm\delta}$ sample with various transition metal ion substitution shows (calcium-doped ceramic oxide) the higher electron mobility and conducting activity.

Address correspondence to E-mail: jrajabathar@ksu.edu.sa; rads12@gmail.com

https://doi.org/10.1007/s10854-023-09986-4

1 Introduction

The unprecedented economic and societal atmosphere may be attributed to the supplies of the big three energy sources such as oil, coal, and natural gas. However, over 60% of the energy released is lost as waste heat energy [1, 2]. All of these issues are driving the demand for obtaining more useful re-use of waste energy. In this context, thermoelectric (TE) material lies within an important niche and has a thematic role to play. TE materials can directly convert heat energy into electricity or play in electric power transformations [3–5]. Ceramic oxide or modified metal oxides could act as thermoelectric property at higher temperature such as 1000 K, for example, strontium titanite, strontium oxide, and calcium cobaltite. Thermoelectric efficiency is described in terms of dimensionless figure of merit ZT values. However, the above-mentioned materials exhibit very low ZT (dimensionless figure of merit) and were reported to be 0.34 at 1000 K by Wunderlich [6, 7]. These complex oxides can be a powerful alternative to conventional thermoelectric based on Bi, Pb, Sb chalcogenides, etc. Since the discovery of thermoelectric properties in $NaCo_2O_4$ (1997), many related cobalt oxides have been synthesized and reported [5, 8–10]. Nowadays, different TE (thermo electric) ceramics are studied as promising candidate for practical TE application. The oxide materials are durable under those conditions of higher temperature and oxidation and have high Seebeck co-efficient with non-toxic properties. The calcium-doped ceramic oxide, $Ca_3Co_4O_{9+\delta}$ is a misfit-layered Co oxides that belong to the family of $[M_mA_2O_{m+2}]^{RS}_q\,[CoO_2]^H$ (M-Co, Bi, Pb, Tl etc.; A-Ca, Sr, Ba; m-0,1,2 (m gives the number of M-cation layers); $q \geq 0.5$(q is called the misfit parameter); possess a layered crystal structure consisting of two types of layer block: a hexagonal $[CoO_2]$ block and a rock salt type $[M_mA_2O_{m+2}]$ block which are stacked along the C-axis forming a composite crystal. In the case of $Ca_3Co_4O_{9\pm\delta}$, (m = 2), it consists of a Ca_2CoO_3 layer having a rock salt structure and a CdI_2 type CoO_2 layer.

Misfit layered cobaltite are promising p-type semiconducting material for TE applications. Further improvement in density and thermoelectric properties is still needed for practical application [11, 12]. TE properties can be improved by improving sintering method or by inventing novel synthesis method [13]. An alternative route is to partially substitute some elements which simultaneously reduce electrical resistivity and thermal conductivity [14]. For practical applications in addition to TE properties and other factors required that are mechanical and magnetic properties, i.e. the material should be sufficiently strong to withstand loads during module life time, so density has to be improved [15]. Li et al., (2021) reviewed the current state-of-the-art material Si/SiGe nanowires in the application of thermoelectric materials [15, 16]. Substitution may affect electron transport properties which all need to be studied in order to improve the thermoelectric behaviour of ceramic oxides. In this work, $Ca_3Co_4O_{9\pm\delta}$ ceramic oxide was prepared by citric acid (CA) ($C_6H_5O_7$) and starch ($C_6H_{10}O_5$)-assisted complex sol–gel combustion method, and thermal hydro-decomposition method and Citric acid-assisted polymer combustion method. Hence, the structural characterization and electrical properties of as-prepared materials have measured in order to study the effect of preparation methods and its thermoelectric properties.

2 Experimental

All chemical is used without further purification from chemical suppliers. In citric acid complex-assisted sol–gel combustion method, stoichiometric amount of metal nitrate solutions is mixed and added into $C_6H_8O_7$ (citric acid) solution with various ratios (Metal ion precursor: CA ratio—1:0.35, 1:0.5, 1:1, 1:1.5, and 1:2). Metal acetate salts were also used. In starch-assisted method, $C_5H_6O_{10}$ (starch) is used instead of citric acid (Metal ion to Starch mole ratio 1:0.5, 1:0.7, 1:1.5). In polymeric combustion method, metal nitrates were mixed with citric acid solution (1:1molar ratio) in ethanol and to this solution, polyethylene glycol (PEG 600) was added. Obtained solutions were evaporated at 393 K to obtain a gel. The gel is dried in an oven at 353 K for 4 h. Dried gel again kept for heating at 623 K. The gel is expanded to a voluminous mass and then collapsed. It was turned into a black material within 4 h. This precursor material was calcined at various temperatures and made pellets using a 12 mm square die. Densities of the pellets were measured after sintering at 1173 K for 24 h by calcination as well as Archimedes method. In thermal hydro-decomposition method, a stochiometric amount of metal acetate salts were taken and made solutions in water and placed in a

furnace. The temperature increased slowly to the calcination temperature. Then pellets were made and sintered.

For the structural characterization, powder X-ray diffraction patterns of the prepared materials were acquired using AXS Bruker D5005 X-ray Diffractometer (Germany) with Cu Kα (λ = 1.5418A°) using Ni filter. The thermal analysis of the precursor was carried out using a differential thermal/thermogravimetric analysis (TG-DSC, TA instrument SDT Q600 V 8.3 Build) in the temperature range from room temperature to 1000° C. Optical properties were recorded on Jasco DR-UV–Visible Spectro photometer V550 ISV 469 between 200 and 800 nm. Electrical properties of the material were analysed by Hall measurement using Ecopia Hall Measurement System (HMS-3000-VER 3.51.5) at room temperature with fixed magnetic field of 0.54 T. Bulk concentration, mobility, average hall co-efficient, and conductivity of the samples were measured.

3 Results and discussion

3.1 Sintered Density and physical parameters' analysis

The as-prepared various route prepared materials were calcined at 1123 K for 12 h and sintered at 1173 K for 24 h. After sintering, the density of the materials was calculated and also measured by Archimedes method. The density was calculated compared to real density of 4.94 g/cm^{-3}, and the densities of the materials were prepared with different molar ratios of metal nitrates to CA, which vary in the range of 2.79–3.28 g/cm^3. The maximum calculated density obtained is 3.28 g/cm^3 for the ceramic oxide with metal ion to CA ratio of 1:2. The corresponding density measured by Archimedes method is 3.62 g/cm^3, which is slightly higher than the calculated as expected. The density of the ceramic oxide is improved by increasing the molar ratio of metal ion:CA. The density of the prepared materials by starch-assisted sol–gel combustion method has also calculated and measured by the Archimedes method.

Hence, the density was found to be increased with decrease in metal ion to starch ratio. The higher density was obtained for Calcium cobalt oxide prepared by starch (CCOS1) with optimized metal ion to starch ratio of 1:0.5. The density obtained is 3.19 g/cm^3 compared to its theoretical density of 64.6%.

The density of the prepared materials by changing stoichiometry ranges from 2.72 g/cm^3 (rel. Density 55%) to 2.91 g/cm^3 (rel. Density 58.9%). The density is found to be improved by decreasing the amount of calcium. The higher density is obtained for $Ca_{2.90}Co_{3.91}O_{9\pm\delta}$, which is 2.91 g/cm^3 (58.9% of theoretical density).

In the case of thermal hydro-decomposition (THD) and polymer method, the density of the material prepared via the polymer combustion method is found to be higher density than that of the material prepared by the thermal hydro-decomposition method. The density obtained is 2.97 g/cm^3 for the polymer combustion method, only 60% of theoretical density. The corresponding Archimedes density is 3.23 g/cm^3, which is 65.4% of theoretical density. Copper nanoparticle doping in metal oxide matrix is very effective for catalysis, and it also enhances the microbial property of the whole matrix [17]. Hence, in the present study, we have also studied the various metal ions that include copper substitution in calcium cobalt oxide thermoelectric material.

The density of the prepared materials by substitution at the Co site calculated and measured by Archimedes method shows that Cu substitution (3.15 g/cm^3, A 3.66 g/cm^3) gives higher density than Fe and Ni substitution (57.3 and 61.9%) of relative density, respectively. The maximum density obtained in each method is given in Table 1.

3.2 Thermal analysis results

The thermogravimetric and differential scanning calorimetric (TG-DSC) analysis of calcium cobalt oxide prepared at 1:2 ratio is shown in Fig. 1. The recorded thermal characterization data for a representative material are shown together in Fig. 1. The TG-DSC curve confirms that the endothermic peak at ∼ 102 °C corresponds to evaporation of residual water present in the precursor material. The endothermic peaks in the range of ∼ 560–700 °C can be assigned to the decomposition of the metal–ligand complex (gel) to form corresponding oxides. The endothermic peak in the range of ∼ 700–800 °C is assigned to the formation of the ceramic material. Thus, the formation of ceramic oxide is confirmed at the calcination temperature of ∼ 850 °C.

Table 1 Sintering methods and variation in its physical parameters

Material	Sintered density (g/cm^3) (A)	Relative density (%)
CCOCA5 (citric acid method)	3.28 (3.62)	66.4 (73.2)
CCOS1(starch-assisted method)	3.19 (3.39)	64.6 (68.6)
CCOCA Polymer (PEG)	2.97 (3.23)	60 (65.4)
CCOTHD (thermal deposition)	2.81 (3.17)	56.8 (64.1)
$Ca_{2.90}$ $Co_{3.91}O_{9+\delta}$ (3.91)	2.91	58.9
$Ca_3Co_{3.8}Cu_{0.2}O_{9+\partial}$	3.15 (3.66)	63.7 (74.1)

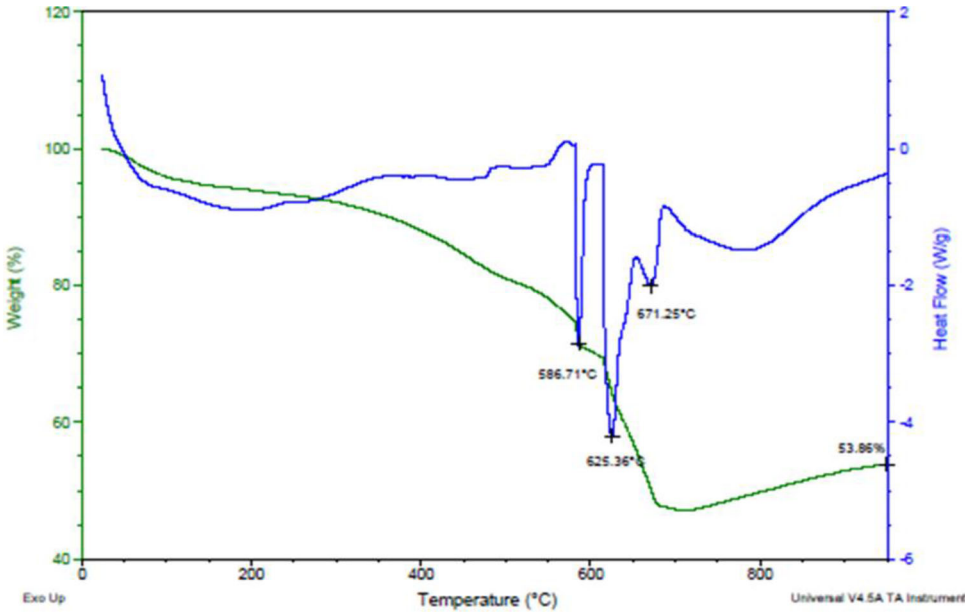

Fig. 1 TG-DSC of the CCOCA5

3.3 Powder X-ray diffraction

The powder X-ray diffraction data recorded for the prepared ceramic oxide material (calc. at 1123 K for 12 h) are presented in Fig. 2 & 3. The reflections in the XRD pattern are matching with the prepared ceramic material as compared with the standard JCPDS file. Thus, the ceramic material formation by complex-assisted sol–gel combustion method is confirmed at the calcination temperature 1123 K.

The defective poor crystalline nature of the as-prepared materials is low sintering at this calcination temperature. The XRD pattern of the material prepared with acetate salts has also confirmed the formation of the ceramic nature at the calcination temperature of 1123 K. Figure 3 shows the much-improved crystalline structure after iron doping in the $Ca_3Co_4O_{9+\delta}$ matrix. The indexed XRD pattern is well matched with reported literature in calcium cobalt oxide thermoelectric ceramic materials [19–23].

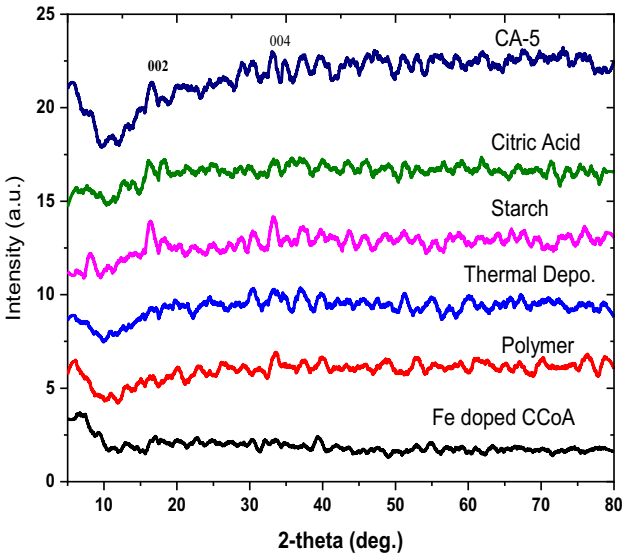

Fig. 2 X-Ray diffraction study of various method-prepared samples ($Ca_3Co_4O_{9+\delta}$ (1–6))

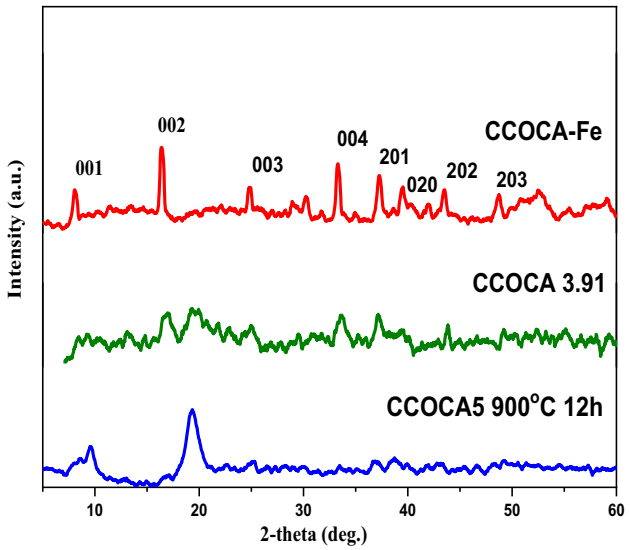

Fig. 3 XRD pattern and effect of Iron doping in $Ca_3Co_4O_{9+\delta}$

3.4 Surface and Electrical properties

The diffuse reflectance (DR)-UV–Visible spectra of the prepared materials are shown in Fig. 4. The spectra contain major peaks around ~ 204 nm and ~ 250 nm and minor broad peak at ~ 340 nm due to the presence of Mg–O, Mn–O. The absorption band obtained in the respective regions is due to the charge transfer transition from the ligand to metal ion doped (LMCT) in this material. Strong absorption bands in the range ~ 700, 500, and 440 cm^{-1} (Fig. 4) show vibration of M–O bonds which prove the decomposition of carbonate at various calcination temperature [18]. The electrical properties of the

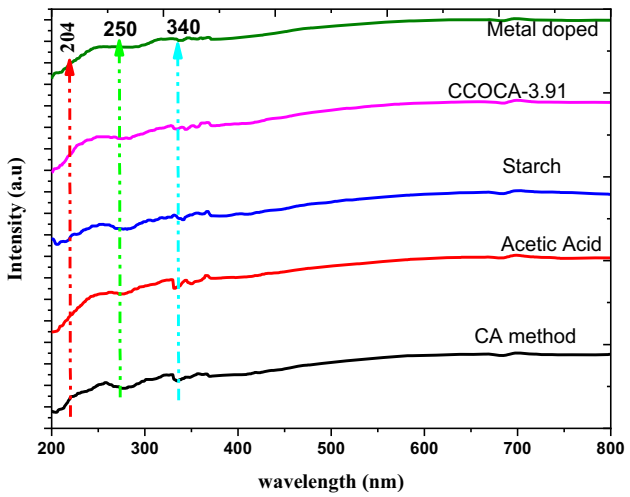

Fig. 4 DR-UV–Visible spectra of various route prepared $Ca_3Co_4O_{9+\delta}$ materials

material were studied using Hall measurement (Table 2). The bulk concentrations of the materials obtained by CA-assisted sol–gel combustion method are in the range of 2–5 × 10^{19} (cm^{-3}). In the case of CCOCA3, the bulk concentration is increased to 35.4 cm^{-3}. The resistivity and conductivity are in the range of 1–2 × 10^2 (Ω cm) and 45–60 (1/Ω cm), respectively [11]. These values are in accordance with the reported data for these types of ceramic materials [19–22]. Further improvement may be possible by modifying the material [12–14]. The variation of the properties such as bulk concentration, mobility, and conductivity is presented in Table 2. Bulk concentration of lower ratio of stoichiometric $Ca_3Co_4O_{9+\delta}$ material shows improved higher conductivity value. No much variation was observed for the other ceramic oxides. As the metal ion:CA ratio increases, mobility is found to be increased in the range 1–14.7 cm^2/Vs [13–17]. The electrical properties of the materials prepared by starch-assisted complex method did not show any remarkable difference than CA method-prepared sample. (Fig. 5)

For the non-stoichiometric route prepared materials, the bulk concentration is in the order of 10^{19} cm^{-3}. Resistivity is in the order of 10–2 Ωcm. Conductivity, bulk concentration, mobility and conductivity is found to be lower for Ca2.90 Co3.91O9+∂ [15–18].

Materials were prepared by polymer combustion method and thermal hydro-decomposition method. In both cases, bulk concentration is in the same order (10^{19} cm^{-3}) and the resistivity in the order of 10^{-2} Ωcm. Conductivity is found to be lower for the material made by polymer combustion method. But the electrical properties are found to be almost same for both the cases. In the case of substitution at the Co site, as expected Cu substitution decreases the bulk concentration and Fe substitution gives increased bulk concentration. Variation in electrical properties by substitution choice at the Co site and its consequences are given in Fig. 6. The bulk concentration of Fe-substituted sample is found to be higher than Ni and Cu-substituted ones (Fig. 6a). Copper-substituted sample shows that the bulk concentration is found to be quite less than the other two. But in the case of conductivity, it is found to be higher for Cu-substituted sample (Fig. 6b). The mobility of Cu-substituted material is found to be quite higher than the other two, and this is because of its low bulk concentration (Fig. 6c). For Fe- and Ni-substituted

Table 2 Electrical properties and Hall measurement analysis

Sample	Bulk concentration (cm^{-3}) × 10^{19}	Mobility cm^2/Vs	Resistivity × 10^{-2} (Ωcm)	Average Hall Co-efficient(cm^3/C)	Conductivity (1/Ωcm)
CCOCA3	35.43	1.05	1.7	0.0176	59.38
CCOCAAc	5.52	5.70	1.9	0.130	50.44
CCO S3	5.31	5.5	2.1	0.116	47.0
$Ca_3Co_{3.91}O_{9+\partial}$	2.21	15.9	1.76	0.281	56.7
CCOTHD1	3.51	7.29	2.4	0.177	41.05
CCOCA polymer	1.68	4.77	7.76	0.370	12.88
$Ca_3Co_{3.8}Fe_{0.2}O_{9+\partial}$	6.010	19.37	1.67	0.3579	54.1

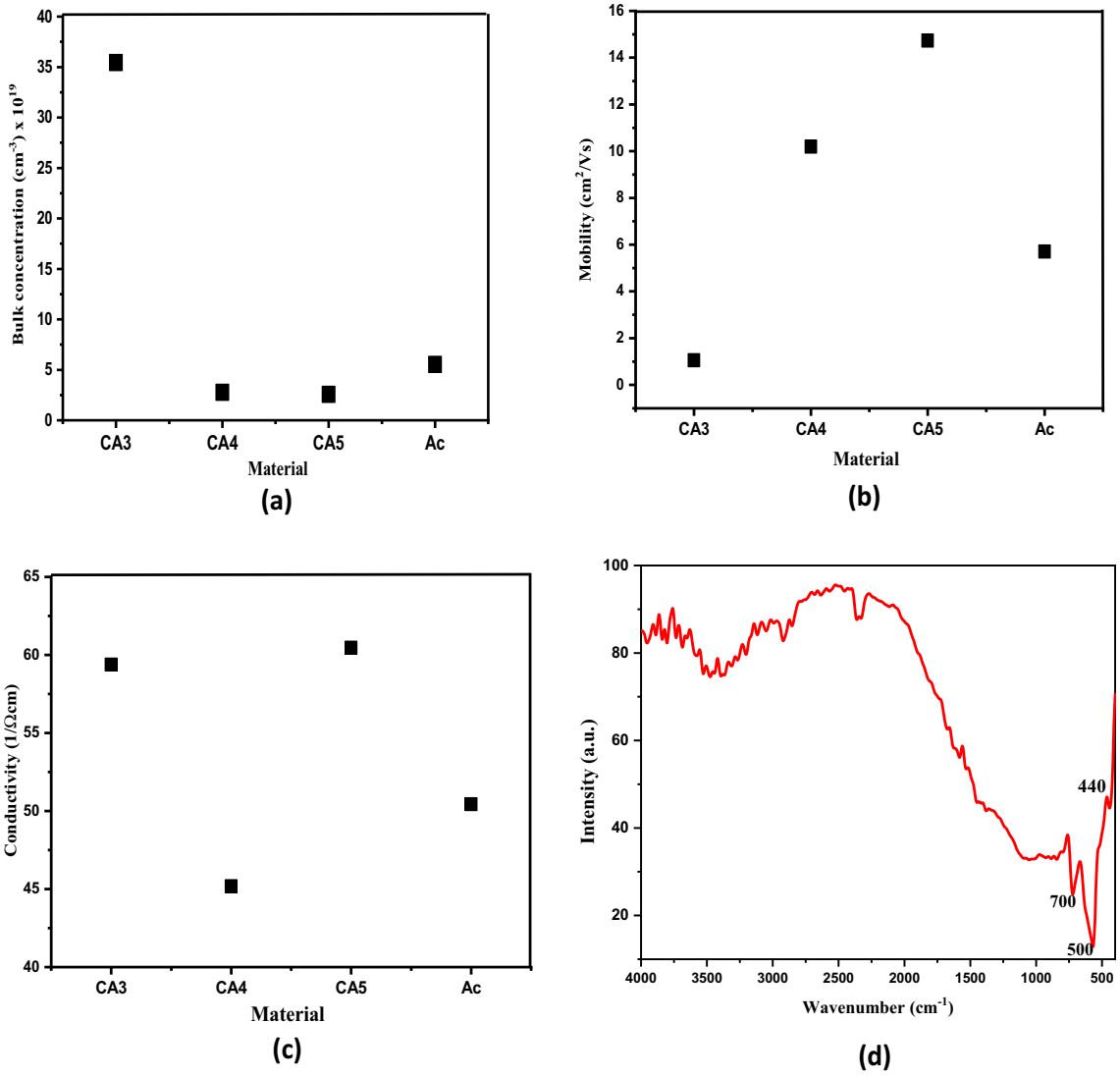

Fig. 5 **a** Variation of bulk concentration, **b** variation of mobility, **c** variation of conductivity and **d** Ft-IR spectra of CCOCA3.91

materials, the mobility found to be almost same. In Co site substitution, Cu incorporation shows higher density (74%, of theoretical density 4.94 g/cm^3) than Ni and Fe substitution. TG-DSC shows complete

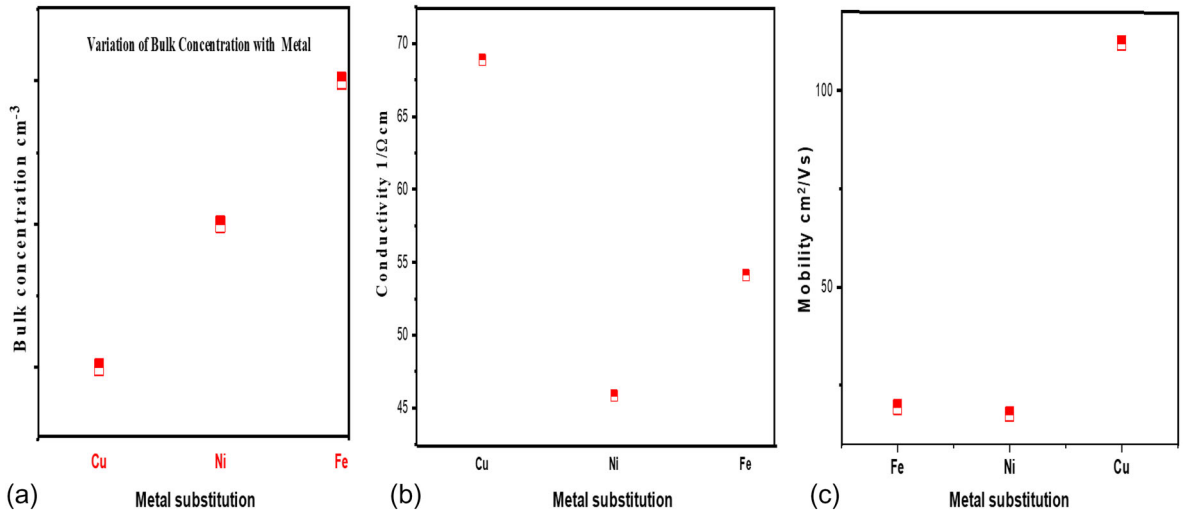

Fig. 6 **a** Variation of Bulk concentration, **b** variation of conductivity, and **c** variation of mobility

decomposition of the formed complex around the calcination temperature of 1123 K. X-ray diffraction pattern shows formation of $Ca_3C\ o_4O_{9+\partial}$ at calc. temp 1123 K [18–22].

However, less crystalline nature suggests the requirement of higher temperature calcination. DR-UV–Visible spectra of all the materials show absorption corresponding to the Ca–O and charge transfer transitions of Co–O in the UV–visible range [23–28]. Hall analysis of the material confirms that the as-prepared $Ca_3Co_4O_{9+\partial}$ **is existed in** p-type. Bulk concentrations of the samples are in the order of 10^{19} $cm^{-3.}$ Resistivity is in the order of 10^{-2} Ωcm. The higher mobility is obtained in the case of hydrothermal method-prepared Calcium cobalt oxide than the other route prepared rest of the materials, which is due to the preparation condition and structural nanorods morphology formation (Fig. 7). Figure 7 A & B shows the high-resolution transmission electron micrograph images of hydrothermal route-prepared iron-substituted $Ca_3Co_4O_{9+\partial}$ p-type materials. The metallic-rich dark particle formation inside the nanorods of the cobalt oxide has visible in the recorded micrographs (red circle marked in Fig. 7). Further, Table 2 shows the variation in hall measurement analysis and mobility property and conductivity data of various method-prepared calcium cobalt ceramic oxides. The materials prepared by thermal hydrothermal deposition, starch-assisted and iron-substituted calcium cobalt oxide are showing promising results in terms of conductivity measurement and electron mobility enhancement (Table 2). Hence, the formation of nanoparticle nature and specific morphology for the calcium cobalt oxide materials could be the key for alteration in their electrical properties' improvement. These electrical mobility and alteration in conducting property could be useful for photocatalysis application by adopting as-prepared metal ions-substituted $Ca_3C\ o_4O_{9+\partial}$ p-type materials towards dye degradation [17, 29–32] and electrochemical sensor application [33, 34].

4 Conclusions

Calcium cobalt oxide (CCO) ceramic materials were synthesized by various reducing agent processes followed by sintering and calcination method. The precursor obtained by citric acid/starch-assisted sol–gel combustion, and polymer combustion and thermal hydro-decomposition method for comparative study of its electrical properties. The density of the prepared materials was measured by theoretical calculation as well as Archimedes method that have demonstrated and the values are obtained in the range of 2.8 to 3.2 g/cm^3; thus, the relative density is obtained around ~ 58–66%. The density found to be higher when the metal ion to CA ratio increased (1:2) and also increased with decrease in metal ion to starch ratio. $Ca_3Co_4O_{9+\partial}$ ceramics was also prepared by changing the stoichiometric amount addition y and by substitution at the Co site. Density was not much improved upon sol–gel chemical preparation. With decrease in amount of Ca, results in density

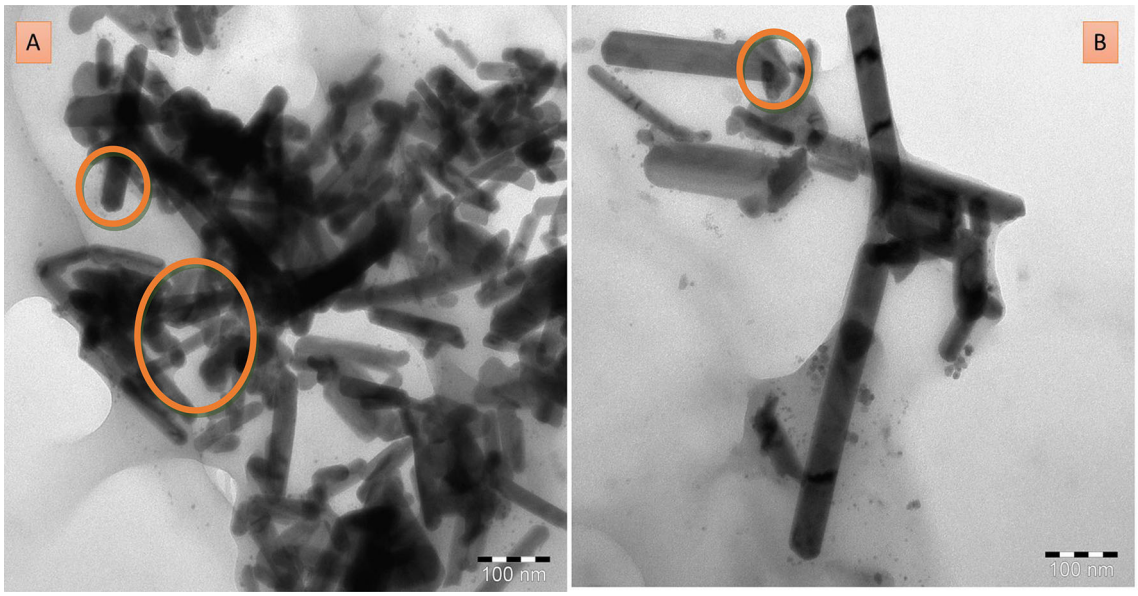

Fig. 7 HR-TEM images of Iron nanoparticle-substituted $Ca_3Co_4O_{9+\partial}$ ceramic oxide prepared by hydrothermal decomposition method (Color figure online)

found to be increased. The $Ca_3Co_4O_{9+\partial}$ samples prepared by polymer method have a higher density than that made by citric acid and starch-assisted method.

Acknowledgements

The authors (RJ and HA) extend their appreciation to the financial support through Researchers Supporting Project number (RSP2023R354), King Saud university, Riyadh 11451, Saudi Arabia.

Author contributions

JRR, development of design of methodology, creation of models, conducting a research work, specifically performing experiments, and data collections. Writing—original draft. RT, formal analysis, validation. HA-L, methodology, formal analysis, writing—review & editing, supervision. HA-S, validation, formal analysis, critical review, commentary and revision, Supervision.

Funding

This work was supported by Researchers Supporting Project number (RSP2023R354).

Data availability

The data that support the findings of this study are available on request from the corresponding author.

Declarations

Competing interests The authors declare that they have no known competing financial interests or personal relationships that could have appeared to influence the work reported in this paper.

Consent to participate The authors agreed that they participating in the research work.

Consent to publish The authors agreed to publish this research paper.

References

1. D. Marxer, P. Furler, J. Scheffe, H. Geerlings, C. Falter, V. Batteiger, A. Sizmann, A. Steinfeld, Demonstration of the entire production chain to renewable kerosene via solar thermochemical splitting of H2O and CO2. Energy Fuels **29**, 3241–3250 (2015). https://doi.org/10.1021/acs.energyfuels.5b00351
2. D. Duan, Y. Zhang, Y. Wang, H. Lei, Q. Wang, R. Ruan, Production of renewable jet fuel and gasoline range hydrocarbons from catalytic pyrolysis of soapstock over corn cob-

derived activated carbons. Energy (2020). https://doi.org/10.1016/j.energy.2020.118454
3. T. Radhika, K.R. Anju, M.S. Silpa, R.J. Ramalingam, H.A. Al-Lohedan, Cellulose acetate/N-TiO2 biocomposite flexible films with enhanced solar photochromic properties. J. Electron. Mater. **46**, 4567–4574 (2017). https://doi.org/10.1007/s11664-017-5442-8
4. T. Radhika, N. Raghu, N. Powrnami, R. Jothi Ramalingam, H.A. Al-Lohedan, Effect of synthesis conditions on formation, electrical properties, and seebeck coefficient of p-type Ca3Co4O9±δ thermoelectric ceramics. J. Electron. Mater. **46**, 1787–1793 (2017). https://doi.org/10.1007/s11664-016-5229-3
5. R.J. Ramalingam, H.A. Al-Lohedan, T. Radhika, Synthesis, surface and textural characterization of ag doped polyaniline-SiO2(Pan-Ag/RHA) nanocomposites derived from biomass materials. Dig. J. Nanomater. Biostructures **11**, 731–740 (2016)
6. Y.F. Wang, K.H. Lee, H. Ohta, K. Koumoto, Fabrication and thermoelectric properties of heavily rare-earth metal-doped SrO(SrTiO3)n (n = 1, 2) ceramics. Ceram. Int. **34**, 849–852 (2008). https://doi.org/10.1016/j.ceramint.2007.09.034
7. M.K. Mohanta, A. Rawat, N. Jena, R. Dimple, A.D. Ahammed, Sarkar, Interfacing boron monophosphide with molybdenum disulfide for an ultrahigh performance in thermoelectrics, two-dimensional excitonic solar cells, and nanopiezotronics. ACS Appl. Mater. Interfaces **12**, 3114–3126 (2020). https://doi.org/10.1021/acsami.9b16866
8. K. Liu, T. Ding, J. Li, Q. Chen, G. Xue, P. Yang, M. Xu, Z.L. Wang, J. Zhou, thermal-electric nanogenerator based on the electrokinetic effect in porous carbon film. Adv. Energy Mater. (2018). https://doi.org/10.1002/aenm.201702481
9. A.S. Santhosh, K.M. Sahana, S. Sandeep, P.N. Prashanth Kumar, N.S. Alsaiari, K.M. Katubi, K.M. Abualnaja, J.R. Rajabathar, Synthesis and application of a 0D/2D nanocomposite for the nanomolar level detection of an antiandrogen drug. New J. Chem. **46**, 16068–16077 (2022). https://doi.org/10.1039/d2nj01967a
10. P. Iyyappa Rajan, J. Judith Vijaya, S.K. Jesudoss, K. Kaviyarasu, S.C. Lee, L. John Kennedy, R. Jothiramalingam, H.A. Al-Lohedan, M. Mahamad Abdullah, Investigation on preferably oriented abnormal growth of CdSe nanorods along (0002) plane synthesized by henna leaf extract-mediated green synthesis. R. Soc. Open Sci. (2018). https://doi.org/10.1098/rsos.171430
11. A.I. Klyndyuk, I.V. Matsukevich, Synthesis and properties of disubstituted derivatives of layered calcium cobaltite. Glass Phys. Chem. **41**, 545–550 (2015). https://doi.org/10.1134/S1087659615050077
12. T. Silva, V. Silva, J. Santos, T. Simões, D. Macedo, Effect of Cu-doping on the activity of calcium cobaltite for oxygen evolution reaction. Mater. Lett. (2021). https://doi.org/10.1016/j.matlet.2021.130026
13. F. Ahmed, A. Munir, A.S. Khan, A.A. Chaudhry, M. Anis-ur Rehman, Facile synthesis and conduction mechanism in re-substituted oxide systems for enhanced thermoelectric performance, J. Mater. Sci. Mater. Electron. **26**(10), 7460–7467 (2015).
14. M.D. Daivajna, N. Kumar, V.P.S. Awana, B. Gahtori, J. Benedict Christopher, S.O. Manjunath, K.Z. Syu, Y.K. Kuo, A. Rao, Electrical, magnetic and thermal properties of Pr0.6-xBixSr0.4MnO3 manganites. J. Alloy. Compd. **588**, 406–412 (2014). https://doi.org/10.1016/j.jallcom.2013.11.033
15. Y. Li, G. Wang, M. Akbari-Saatlu, M. Procek, H.H. Radamson, Si and SiGe nanowire for micro-thermoelectric generator: a review of the current state of the art. Front. Mater. **8**, 1–24 (2021). https://doi.org/10.3389/fmats.2021.611078
16. Chinese Materials Conference on Materials and Technologies for Energy Supply and Environmental Engineering, 2015, Mater. Sci. Forum. 847 (2016) 1–546. https://www.scopus.com/inward/record.uri?eid=2-s2.0-84962182347&partnerID=40&md5=b5f76c6bc5be7b0f9af9d4db6eea6e13.
17. R. Jothiramalingam, S. Devasanan, H.A. Lohedan, M.R. Muthumareeswaran, H.M. Alqahtani, K. Abdalnaser, Green chemistry method prepared effective copper nanoparticles by lemon flower (citrus) extract and its anti-microbial activity. Dig. J. Nanomater. Biostr. **17**, 145–151 (2022)
18. M.U. Sajid, H.M. Ali, Thermal conductivity of hybrid nanofluids: a critical review. Int. J. Heat Mass Transf. **126**, 211–234 (2018). https://doi.org/10.1016/j.ijheatmasstransfer.2018.05.021
19. G. Constantinescu, M.A. Sh Rasekh, M.A. Torres, J.C. Diez, M.A. Madre, A. Sotelo, Effect of Sr substitution for Ca on the $Ca_3Co_4O_9$ thermoelectric properties.". J. Alloy. Compd. **577**, 511–515 (2013)
20. J.C. Diez, M.A. Torres, S. Rasekh, G. Constantinescu, M.A. Madre, A. Sotelo, Enhancement of $Ca_3Co_4O_9$ thermoelectric properties by Cr for Co substitution. Ceram. Int. **39**(6), 6051–6056 (2013)
21. M.A. Torres, F.M. Costa, D. Flahaut, K. Touati, Sh. Rasekh, N.M. Ferreira, J. Allouche, M. Depriester, M.A. Madre, A.V. Kovalevsky, J.C. Diez, A. Sotelo, Significant enhancement of the thermoelectric performance in $Ca_3Co_4O_9$ thermoelectric materials through combined strontium substitution and hot-pressing process. J. Eur. Ceram. Soc. **39**(4), 1186–1192 (2019)
22. Sh. Rasekh, M.A. Torres, G. Constantinescu, M.A. Madre, J.C. Diez, A. Sotelo, Effect of Cu by Co substitution on

$Ca_3Co_4O_9$ thermoelectric ceramics. J. Mater. Sci.: Mater. Electron. **24**(7), 2309–2314 (2013)
23. D. Kenfaui, D. Chateigner, M. Gomina, J.G. Noudem, Texture, mechanical and thermoelectric properties of $Ca_3Co_4O_9$ ceramics. J. Alloy. Compd. **490**(1–2), 472–479 (2010)
24. M.A. Torres, G. Garcia, I. Urrutibeascoa, M.A. Madre, J.C. Diez, A. Sotelo, Fast preparation route to high-performances textured Sr-doped $Ca_3Co_4O_9$ thermoelectric materials through precursor powder modification. Sci. China Mater. **62**(3), 399–406 (2019)
25. H. Fukutomi, Y. Konno, K. Okayasu, M. Hasegawa, H. Nakatsugawa, Texture development of $Ca_3Co_4O_9$ thermoelectric oxide by high temperature plastic deformation and its contribution to the improvement in electric conductivity. Mater. Sci. Eng. A **527**(1–2), 61–64 (2009)
26. A. Sotelo, G. Constantinescu, Sh. Rasekh, M.A. Torres, J.C. Diez, M.A. Madre, Improvement of thermoelectric properties of $Ca_3Co_4O_9$ using soft chemistry synthetic methods. J. Eur. Ceram. Soc. **32**(10), 2415–2422 (2012)
27. M.A. Madre, S. Rasekh, M.A. Torres, J.C. Diez, A. Sotelo, Improving bulk $Ca_3Co_4O_9$ thermoelectric materials through Zr doping. Adv. Appl. Ceram. **117**, 142–146 (2018). https://doi.org/10.1080/17436753.2017.1386409
28. F. Delorme, C.F. Martin, P. Marudhachalam, D. Ovono Ovono, G. Guzman, Effect of Ca substitution by Sr on the thermoelectric properties of $Ca_3Co_4O_9$ ceramics. J. Alloy. Compd. **509**, 2311–2315 (2011). https://doi.org/10.1016/j.jallcom.2010.10.209
29. K. Obata, Y. Chonan, T. Komiyama, T. Aoyama, H. Yamaguchi, S. Sugiyama, Grain-oriented $Ca_3Co_4O_9$ thermoelectric oxide ceramics prepared by solid-state reaction. J. Electron. Mater. **42**(7), 2221–2226 (2013)
30. M. Sundararajan, J. Vidhya, R. Revathi, M. Sukumar, B. Arunadevi, R. Rajkumar, S. Ramachandran, M. Kamalakannan, C.S. Dash, J.R. Rajabathar, Rapid synthesis and magnetic property characterization of Mg^{2+} doped Co_3O_4 nanostructures. Inorg. Nano-Metal Chem. (2022). https://doi.org/10.1080/24701556.2021.2025400
31. P.S. Selvamani, J.J. Vijaya, L.J. Kennedy, A. Mustafa, M. Bououdina, P.J. Sophia, R.J. Ramalingam, Synergic effect of Cu2O/MoS2/rGO for the sonophotocatalytic degradation of tetracycline and ciprofloxacin antibiotics. Ceram. Int. **47**, 4226–4237 (2021)
32. J.R. Rajabathar, J.R. Rajabathar, H.A. Al-Lohedan, S. Arokiyaraj, Z.A. Issa, C.S. Dash, S. Murugesan, S.K.K. Pasha, D.M. Al-dhayan, J.N. Appaturi, Characterization of pure rutile titania nanoparticle prepared by feasible method for coatings and visible light-driven dye removal application. Coatings (2021). https://doi.org/10.3390/coatings11101150
33. M. Govindasamy, S.-F. Wang, R. Jothiramalingam, S. Noora Ibrahim, H.A. Al-lohedan, A screen-printed electrode modified with tungsten disulfide nanosheets for nanomolar detection of the arsenic drug roxarsone. Microchim. Acta. (2019). https://doi.org/10.1007/s00604-019-3535-1
34. M. Govindasamy, S.-F. Wang, W.C. Pan, B. Subramanian, R.J. Ramalingam, H. Al-lohedan, Facile sonochemical synthesis of perovskite-type $SrTiO_3$ nanocubes with reduced graphene oxide nanocatalyst for an enhanced electrochemical detection of -amino acid (tryptophan). Ultrason. Sonochem. **56**, 193–199 (2019)